行政院國家科學委員會專題研究計畫　期中進度報告

二維無序或關聯電子系統狀態之理論研究(2/3)

計畫類別：個別型計畫
計畫編號：NSC94-2112-M-032-001-
執行期間：94 年 08 月 01 日至 95 年 07 月 31 日
執行單位：淡江大學物理學系

計畫主持人：何昌明

報告類型：精簡報告

處理方式：本計畫可公開查詢

中　華　民　國 95 年 6 月 21 日

Project Progress Report

Chang-Ming Ho
Dept. of Physics, Tamkang University
May 31, 2006

What we have achieved this year in our two papers, one just submitted to Phys. Rev. Lett. and one appeared in J. Phys. Chem. Solids, and other on-going work will be discussed in this report. This year, we focus on understanding the phenomena observed in applying spectroscopy probes-scanning tunneling spectroscopy (STS) on high *Tc* cuprates in terms of the many-particle trial wave functions (TWFs) [see section (I) below]. The published paper is a summary of our continuous efforts in comparing the trial-wave–function approach with the results of angle-resolved photoemission spectroscopy (ARPES) [see section (II) below]. Working with my assistants, we have also started to investigate other 2-dimensional systems, such as the recently made graphene and a Manganite thin film, $La_{1-x}Zr_xMnO_3$, showing colossal magneto-resistance (see section (III) below). In the following, we discuss the work in more detail.

(I) Understanding the recent STS on cuprates- numerical and analytic study:

To understanding the nature of the superconducting state in cuprates, we have been concerning about phenomena seen in the STS which provides information for the electronic states in real space. While ARPES probes, in short, the spectral function $A(\mathrm{k},\omega)$, the STS, by measuring the derivative of the tunneling current, *dI/dV*, at each position, r, probes the properties of the same function at each position on the sample surface [1], *i.e.*

$$A_{\mathrm{s}}(\mathrm{r},\omega)=\sum_m \left\langle 0\left|c_{\mathrm{r}}^{+}\right|m\right\rangle\left\langle m\left|c_{\vec{0}}\right|0\right\rangle\delta(\omega+E_m-E_0)+\sum_m \left\langle 0\left|c_{\mathrm{r}}\right|m\right\rangle\left\langle m\left|c_{\vec{0}}^{+}\right|0\right\rangle\delta(\omega-E_m+E_0),$$

where $|0\rangle$ is the ground state of the system at some particular doping. Recent scanning tunneling microscopy/spectroscopy (STM/STS) results have shown that there are all varieties of phenomena existed in different high *Tc* cuprates with easily-cleaved surfaces- *e.g.* inhomogeneous distribution of gaps (in between the tunneling peaks) [2] and quasi-particle scattering at low energy in Bi2212 [3], checker-board like patterns in *dI/dV* at low sample bias in $Ca_{2-x}Na_xCu_2OCl_2$ [4], asymmetry of *dI/dV* at positive (electron injected) and negative (hole injected) bias [5], and so on.

The attempt to understand the features seen in STM/STS *hitherto* is mainly on the effects of the inhomogeneous dopant induced SC order parameters to the local density of states (LDOS) of

the *d*-wave BCS (*d*-BCS) state [6]. While the anti-correlation between LDOS peak heights and gap sizes is indeed found there, the strong correlation between electrons which should be important in underdoped cuparets is completely neglected [7]. Recently, Anderson proposed that the asymmetric tunneling conductance is closely related to the strong correlations inherent in the Gutzwiller projection of the resonating-valence-bond wave function (RVB WF) [8]. However, there have been controversy whether the asymmetry is accounted for by the coherent quasi-hole (-particle) excitations of the projected state treated by the usual approximation scheme of the renormalized mean-field theory (RMFT) [9] or rather by the incoherent part dictated by the spectral sum rule [10]. Also, the correlation between gap sizes and peak heights has not yet been examined properly with the strong correlation explicitly included.

Motivated by the work of Anderson [8], we examine exactly the effects of strong correlation by numerically investigating the low-energy spectral weights of the *d*-wave RVB (*d*-RVB) state on finite square lattices. More precisely, we calculate the spectral weights (with N the total electron number) $Z_{\mathrm{k}}^{+} \equiv \left|\left\langle \Psi_{N+1}\left|c_{\mathrm{k}}^{+}\right|\Psi_{N}\right\rangle\right|^{2} /[\left\langle \Psi_{N+1}\middle|\Psi_{N+1}\right\rangle\left\langle \Psi_{N}\middle|\Psi_{N}\right\rangle]$ and

$$Z_{\mathrm{k}}^{-} \equiv \left|\left\langle \Psi_{N-1}\left|c_{\mathrm{k}}\right|\Psi_{N}\right\rangle\right|^{2} /[\left\langle \Psi_{N-1}\middle|\Psi_{N-1}\right\rangle\left\langle \Psi_{N}\middle|\Psi_{N}\right\rangle]$$

which correspond to adding and removing one electron to and from the ground state with particular doping of holes, respectively, where $\left|\Psi_{N+1}\right\rangle \equiv P_d c_{\mathrm{k}}^{+}\left|\Psi_{N}\right\rangle_0$ is the trial WF for the quasi-particle excitation for momentum $\mathrm{k}[\equiv(k_x,k_y)]$ and $\left|\Psi_{N-1}\right\rangle \equiv P_d c_{\text{-k}}^{+}\left|\Psi_{N-2}\right\rangle_0$ for the quasi-hole excited states. The ground state $\left|\Psi_{N}\right\rangle = P_d\left|\Psi_{N}\right\rangle_0 \equiv P_d(\sum_{\mathrm{q}} a_{\mathrm{q}} c_{\mathrm{q}}^{+} c_{-\mathrm{q}}^{+})^{N/2}\left|0\right\rangle$ which is the variationally optimized *d*-RVB state. Here, the usual coherent factor $a_{\mathrm{k}} \equiv v_{\mathrm{k}}/u_{\mathrm{k}} = \Delta_{\mathrm{k}}/(\varepsilon_{\mathrm{k}} + \sqrt{\varepsilon_{\mathrm{k}}^2 + \Delta_{\mathrm{k}}^2})$, where $\Delta_{\mathrm{k}} = \Delta_v(\cos k_x - \cos k_y)$ the *d*-wave pairing amplitude and $\varepsilon_{\mathrm{k}} = -2t_v(\cos k_x + \cos k_y) - 4t_v'\cos k_x \cos k_y - 2t_v''(\cos 2k_x + \cos 2k_y) - \mu$ the electron dispersion. The operator P_d projects out the double-occupied sites in the system with finite number of doped holes. We have four variational parameters $(\Delta_v, \mu, t_v', t_v'')$ in which t_v' and t_v'' are associated with the long-range hopping in the *t-t'-t"-J* model Hamiltonian,

$$H = -\sum_{i,j} P_d t_{ij}(c_i^{+} c_j + \text{Hermitian conjugate}) P_d + J\sum_{\langle i,j\rangle}(\vec{S}_i \cdot \vec{S}_j - \frac{1}{4} n_i n_j),$$

where hopping amplitude $t_{i,j} = t$, *t'* and *t"* for sites *i* and *j* being the nearest, the next-nearest and

the third-nearest neighbors, respectively. $\vec{S}_i$ the spin operator at site *i* and <*i*,*j*> means that the interaction between spins occurs only for nearest-neighbor sites.

Applying the identities for projection operator, we can relate Z_{k}^{+} exactly to the momentum distribution function n_{k} as $Z_{\mathrm{k}}^{+} = [(1+x)/2] - n_{\mathrm{k}}$, where *x* is the density of doped holes and $n_{\mathrm{k}} = \langle \Psi_N | c_{\mathrm{k}}^{+} c_{\mathrm{k}} | \Psi_N \rangle / \langle \Psi_N | \Psi_N \rangle$. While there is no exact relation like this for Z_{k}^{-}, we find an interesting relation between $P_{\mathrm{k}} \equiv Z_{-\mathrm{k}}^{+} Z_{\mathrm{k}}^{-}$ which represents the off-diagonal long-range order in the pairing correlation and the *d*-wave pairing order parameter Δ_{op} by

$$\Delta_{op} = (2/N) \sum_{\mathrm{k}} \left| \cos k_x - \cos k_y \right| \sqrt{P_{\mathrm{k}}} \ .$$

We computed both the spectral weights numerically and found the doping dependence of Δ_{op} indeed has the dome-like shape, similar to the *Tc* versus doping determined experimentally. (See Fig.1 at the end of this report. The lattice size is 12×12 there.) Actually, the peak positions shown in Fig.1 are almost the same as what have been obtained previously by studying the *d*-wave long-range pair-pair correlation [11]. The reduction of SC order parameter after that doping level is mainly caused by Z_{k}^{-} around the anti-nodal region, reminiscent of the decreasing of long-range correlation due to the Fermi surface geometry in the same momentum space [11]. Hence the relation we found provides another way to evaluate the strength of the pairing amplitude.

We then recognize that the strong correlation effects becomes apparent only in the electron removing spectral weight at low doping, reminiscent of what have been shown previously by analytic approach [12]. The effects due to strong correlations are examined by comparing the coherent spectral weights averaged over all momenta, *i.e.* $Z_{ave}^{-} \equiv \sum_{\mathrm{k}} Z_{\mathrm{k}}^{-} / N$ and the incoherent part defined by the relation $n_{ave}^{incoh} \equiv n_{ave} - Z_{ave}^{-}$ obtained by exact treatment of the projection and RMFT. Here $n_{ave} \equiv \sum_{\mathrm{k}} n_{\mathrm{k}} / N$ is the average momentum distribution function which should be given always by the electron density of the system. The exact results for the 12×12 lattice and that by RMFT are shown in Fig.2. As is shown there, while numerical n_{ave} (solid circles) is

indeed equal to the electron density, the exact incoherent spectral weights for electron removal is less than the RMFT result. The difference becomes more significant as hole doping level is reduced. Interestingly, this behavior is independent of the $(t',t'')/t$ values (represented by solid and empty symbols in Fig.2) which correspond to very different doping dependence of the Fermi surface shape and also the DOS. By contrast, the average values of electron adding spectral weights calculated exactly (not shown) and by RMFT are identical due to the exact relation

between Z_{k}^{+} and n_{k} discussed above.

We then move to concentrate on the spectral weights as a function of the excited-state energy to make a comparison with tunneling experiments. By applying the model Hamiltonian to excitations $\left|\Psi_{N\pm1}\right\rangle$, we deduce their excitation energies for each momentum and also the corresponding energy gap Δ by fitting the excitation energy. To reduce the effects of finite systems, we define the sum of $Z_{\mathrm{k}}^{\pm}/N$, over momentum k which has energy within some appropriate energy interval ΔE, to be the low-energy average spectral weight, $Z_L^{\pm}(E)$, with E the mid value of the chosen ΔE. Taking $Z_L^{\pm}(E)$ as an approximation to the spectral function at low energy, we plot $Z_L^{\pm}(E)$, in Fig.3, up to where peaks appear for lattices of size 12×12 with ΔE =0.3, and also 20×20 with energy interval 0.2 for various dopings. To make sure our treatment is correct, we have also applied the same analysis to the *d*-BCS state (*i.e.* without projection). As shown in the inset of Fig.3, the ideal BCS result is hardly distorted by the finite size. Note that, with the reasonable finite-size dependence we obtain indeed the *V*-shape *d*-wave gap near zero energy. The width between peak positions is also roughly equal to two times of the gap value deduced from the excitation energy. Looking at the result closely, while the the amplitudes of the average weights may indeed be about the same at the very neighbors of zero energy as suggested by others [13], the average weights $Z_L^{-}(E)$ are always larger than that of $Z_L^{+}(E)$ at energy near that of peak. With decreased doping, the ratio of the average spectral weight values at negative and positive energies enhances quite dramatically, *e.g.* from *x*=0.125 to 0.056, $Z_L^{-}(-\Delta)/Z_L^{+}(\Delta)$ at the corresponding energy of the peak Δ increases from 1.96 to 2.73. Similar behaviors are found for the case with vanishing $(t',t'')/t$ (not shown). In contrast to this, in the *d*-BCS (inset in Fig.3) in the same finite lattices there is almost no change of the ratio within the gap. The numerical results remind us the particle-hole asymmetric average conductance and the enhancement of the asymmetry with underdoping observed in the

spectroscopy measurement.

Fig.3 also reveals correlation between heights of the spectral weight peak and the gap size (or the width between peaks) as doping level is varied. Within the doping level shown in Fig.4, the peak height scales with the pairing amplitude but apparently anti-correlates with the gap size. This is in clear contrast to the BCS case in which the peak height, proportional to the SC coherence, scales with the width between peaks or gap size as more holes doped into the system. Our result agrees qualitatively with what has been extracted from STS experiments [1-5]. It should be noted that our result demonstrates that the width between Z_{k}^{+} and Z_{k}^{-} for a strongly correlated system is determined by the excitation gap in the SC state.

This concludes the discussion on our numerical study on tunneling into the cuprates. This work is in collaboration with with Prof. T.K. Lee (Academia Sinica) and his student Mr. Chun-Pin Chou (National Tsing Hua University and Academia Sinica). A paper on this has been submitted to

Phys. Rev. Lett. in May, 2006. It is now reviewed by the referees.

Related to the tunneling phenomena, I have been working with Prof. M. Ogata (University of Tokyo) following the Gutzwiller projection approximation put forward by Laughlin recently to examine analytically the (partial) projection of non-double occupancy on the BCS state [14]. To keep the electron density the same as the projection strength is varied, a parameter called fugacity factor is included in the constructed WF. Turning on the projection, the *d*-wave superconducting state is associated with only a tiny superfluid density near half-filling (or zero doping) due to the on-site repulsion- thus called "gossamer" superconductivity (gSC). Intriguingly, there exists quasi-particle state of the gSC pinned within the “Hubbard-like” charge gap.

To examine the tunneling asymmetry issue, we may first calculate the spectral weights mentioned above. However, we found that Z_{k}^{-} and Z_{k}^{+} are actually identical with or without the fugacity factor, as shown by Fukushima *et al* [10]. We therefore construct a new trial excited state $\left|\Psi_{N-1}\right\rangle$ by introducing an additional parameter g that characterizes the weight of doubly occupied site (explicit form not shown here). It is then found that, applying the Gutzwiller approximation scheme, the asymmetry does appear in the spectral weights $Z_{\mathrm{k}}^{\pm}(g)$, now functions of g, as a specific g is determined by minimizing the excited-state energy. *The preliminary result has been reported by Prof. Ogata in the Autumn meeting of the Japanese Physical Society in 2005.* We are continuing to examine related issues with this new trial WF.

(II) Trial WF versus ARPES results:

In the past year, we continue to apply the trial excited state of RVB WF to understand features seen in recent ARPES experiments. In our paper published in *Journal of Physics and Chemistry of Solids* [vol. 67, p.150 (2006)], we discuss briefly our work of applying the trial WF's with and without antiferromagnetic order for the *t-J*-type model proposed to describe the low-energy states of high *Tc* cuprates with doped holes or electrons. More precisely, we review that, in the slightly doping regime, the ground states behave like charged quasi-particles with well-defined momenta and have much less pairing correlations than previously studied ones. There exist also states showing the incoherent and "spin-bag" behaviors. Our results are supported by exact calculation and are consistent with recent photoemission experiments. We then showed that the superconducting states indeed emerge as hole doping is increased. The superconducting pairing strength behave similarly with the long-range hopping amplitudes described in recent band-structure analysis. [15]

We have been trying to extend the numerical study on the spectral weights to the transfer of them at particular momenta as the state changes from the normal (projected Fermi liquid and so on) to the superconducting (RVB). As revealed most clearly in recent optical conductivity experiment,

the spectral weight transfer in various high *Tc* cuprates as they becomes superconducting (and thus the gap opens) extends up to very high energy, different from that occurs in the low *Tc* materials. More specifically, we would like to examine this issue by comparing the situations for the Fermi liquid to *d*-wave BCS and the case between projected ones. It is then possible to compare results of our study and of ARPES on particular kind of cuprates (maybe single-layer ones with lower *Tc*). This work is again in collaboration with Mr. Chun-Pin Chou (National Tsing Hua University; Academia Sinica) and T.K. Lee (Academia Sinica).

(III) Study on other Two-dimensional systems:

With my assistants, one graduate and two undergraduate students, we are exploring other two-dimensional systems. They include a non-interacting electron systems with honeycomb lattice, graphene sheets (namely, single-layer component of the graphite), only recently available and have attract a lot of attention; and a Manganite thin film system, $La_{1-x}Zr_xMnO_3$, for which two of my undergraduate assistants are doing related experiments with my colleague at Tamkang.

(i) Recently, quantized Hall effect is observed in the graphene sheet [16]. Unlike the previously studied two-dimensional systems and quasi-one-dimensional organic systems, graphene sheet has a unique property that there exist zero modes (so-called massless Dirac Fermions) without a magnetic field at half-filling due to the honeycomb lattice structure. Hall conductivity in graphene has been observed to be $(2+4n)(e^2/h)$, where n is an integer. These unusual quantized

Hall effect have been explained as a result of 4 times the quantum Hall conductivity $[(1/2)+n](e^2/h)$ for each Dirac Fermions, where the factor 4 comes from the spin degree of freedom times number of the Dirac Fermions in the Brillouin zone. The spin orbit interaction introduces a gap in the spectrum and may produce interesting phenomena [17].

We notice that it is possible to understand the physical properties of the graphene sheet in terms of the "supersymmetric" quantum mechanics, as have been done recently [18] without spin orbit interactions. We would like to apply the property of the "shape-invariant potential" in this approach [19] to study the effects of, for example, including the spin orbit interactions. Also, we would like to examine the aspects of Berry phases in the system.

(ii) As for another system we have been looking at is the $La_{1-x}Zr_xMnO_3$ in a thin film form. In this system, some of the *La*3+ ions is substituted by tetravalent ions, *Mn*3+ ions will be deoxidized into *Mn*2+ ions, which is equivalent to introducing electrons into the e_{2g} band.

Effects of tetravalent ion doping, including*Ce*4+, *Zr*4+, *Sn*4+ and *Te*4+, have been studied extensively (see [20] and refernences therein). It is reported that the *Ce*-doped system studied by photoemission/x ray absorption spectroscopy and Hall effect indeed show electron-doped nature. To explain the strong magnetic–resistive correlation in the electron-doped Manganites, the presence of double-exchange between *Mn*2+ and *Mn*3+ has been proposed. Recently, however, some groups have found that the film was actually hole doped, not electron doped. All these indicate that the character of the charge carriers in *Ce* doped Manganites is under debate. To clarify the debate, it is necessary to further study other tetravalent ion-doping Manganites. However, it is claimed in recent study that the charge carrier in the *Zr* doped thin film is still of the hole-like character [20]. It is argued that the presence of cation vacancies counteracts the effect of *Zr*4+ ions, resulting in a hole-doping effect. When the average valence of Mn was less than 3+, *i.e.*, the sample was truly electron doped, *no* magnetic–resistive correlation was observed.

My colleague, Prof. Dah-Chin Ling, and his group have been working on the $La_{1-x}Zr_xMnO_3$ thin film on different substrates [21]. To clarify the issue on the doped carrier and the physical properties of this thin-film system, two undergraduate assistants of mine have been trying to examine more samples under different conditions with the help of Prof. Ling and his graduate students. Within this summer, we shall be able to collect results and then make analysis on that.

Bibliography

[1] K. McElroy, *et al.*, arXiv; cond-mat/0505333.

[2] K.M. Lang *et al.*, Nature 415, 412 (2002).

[3] J.E. Hoffman, *et al.*, Science 297, 1148 (2002); K. McElroy, *et al.*, Nature 422, 422, 592 (2003).

[4] T. Hanaguri *et al.*, Nature 430, 1001 (2004)

[5] C. Renner and ∅. Fischer, Phys. Rev. B 51, 9208 (1995); T. Hanaguri, private communication.

[6] See, for example, T. S. Nunner *et al.*, Phys. Rev. Lett. 95, 177003 (2005); M. Cheng and W. P. Su, Phys. Rev. B 72, 094512 (2005).

[7] P. A. Lee, N. Nagaosa and X.-G. Wen, Rev. Mod. Phys. 78, 17 (2006).

[8] P.W. Anderson and N. P. Ong, J. Phys. Chem. Solids 67, 1 (2006); see also cond-mat/0405518.

[9] F. C. Zhang *et al.*, Supercond. Sci. Tecnnol. 1, 36 (1988).

[10] M. Randeria *et al.*, Phys. Rev. Lett. 95, 137001 (2005); N. Fukushima *et al.*, Phys. Rev. B72, 144505 (2005).

[11] C.T. Shih *et al.*, Phys. Rev. Lett. 92, 227002 (2004).

[12] W. Rantner and X.-G. Wen, Phys. Rev. Lett. 85, 3692 (2000).

[13] H.-Y. Yang *et al.*, arXiv: cond-mat/0604488.

[14] R. B. Laughlin, arXiv: cond-mat/0209269.
[15] E. Pavarini *et al*., Phys. Rev. Lett. 87, 047003 (2001).
[16] K.S. Novoselov *et al.*, Nature 438, 197 (2005); Y. Zhang *et al.*, Nature 438, 201 (2005).
[17] C.L. Kane and E. J. Mele, Phys. Rev. Lett. 95, 226801 (2005).
[18] M. Ezawa, arXiv: cond-mat/0606084.
[19] R. Dutt, A. Khare and U. P. Sukhatme, Am. J. Phys. 56, 163 (1988).
[20] D. J. Wang *et al.*, J. Phys.: Condens. Matter 18, 741 (2006).
[21] Y.-W. Chou (周翊瑋), *Strain Effects on the Structure and Magneto-transport Properties of* $La_{0.85}Zr_{0.15}MnO_3$ *thin film*, Master Thesis, unpublished (Tamkang University, 2004).

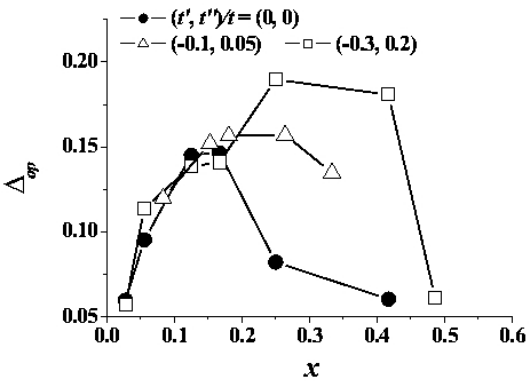

Fig.1

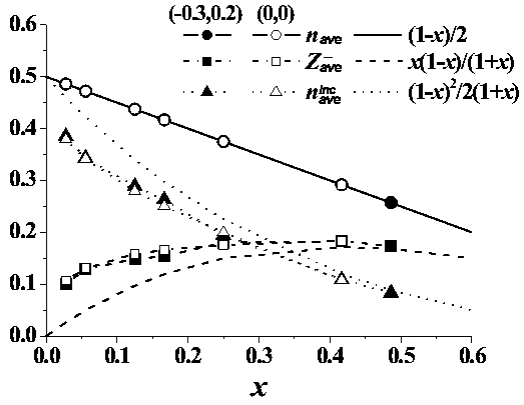

Fig.2

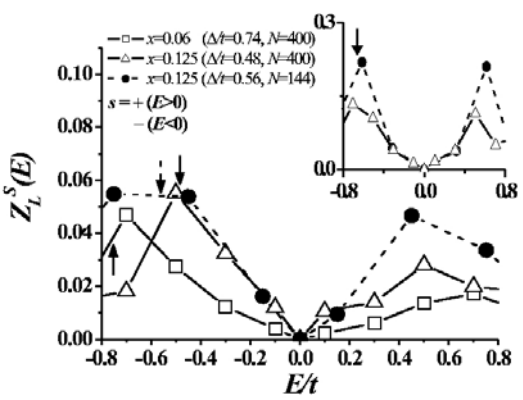
x=0.06 (Δt=0.74, N=400)
x=0.125 (Δt=0.48, N=400)
x=0.125 (Δt=0.56, N=144)
s = + (E>0)
– (E<0)
$Z_L^s(E)$
E/t

Fig.3

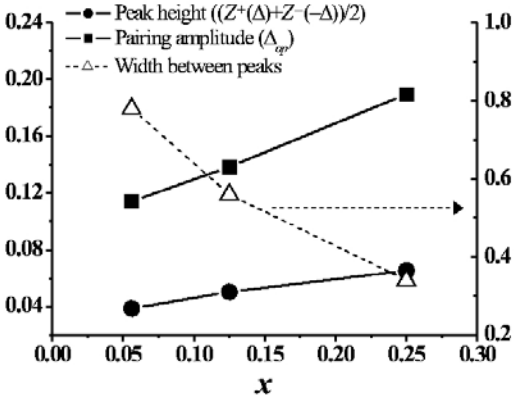
Peak height ((Z⁺(Δ)+Z⁻(–Δ))/2)
Pairing amplitude (Δ_{qp})
Width between peaks
x

Fig.4